Scaling Laws for Strongly Anharmonic Vibrational Matrix Elements

M. S. Child,* M. P. Jacobson,† and C. D. Cooper

Physical and Theoretical Chemistry Laboratory, South Parks Rd, Oxford, OX1 3QZ, UK

Received: July 9, 2001; In Final Form: September 12, 2001

The Heisenberg correspondence between classical Fourier components and quantal matrix elements is used to demonstrate remarkably accurate scaling laws, by which the matrix elements scale simply with the reduced energy ($\bar{E}/B$), where B is a characteristic energy parameter and $\bar{E}$ is the average energy of the relevant states. Applications to the Morse oscillator, a cylindrically symmetric double well (champagne bottle) potential and to the spherical pendulum are described. The relevance of the scaling rules to modeling highly excited molecular vibrational states close to saddle points on the potential surface is discussed. Significant differences between Morse oscillator and vibron oscillator matrix elements are reported.

I. Introduction

Resonant energy flow in polyatomic molecules continues to attract substantial experimental and theoretical interest, particularly the interplay between "chaos" and localization at high vibrational excitation, and its implications for mode selective chemistry. A simple but powerful class of models for studying resonant vibrational dynamics (from quantum, classical and semiclassical viewpoints) is based on effective Hamiltonians, which may either be parametrized to reproduce experimental data or derived from ab initio potential energy surfaces by perturbation theory.[1,2] In either case most current models are expressed, implicitly or explicitly, as expansions in harmonic oscillator shift operators. In other words the quantum (and, by the correspondence principle, classical action angle) dynamics are fundamentally based on harmonic oscillator scaling rules, which are particularly simple, because it is always possible to separate the spectroscopic parameters from the quantum numbers. For example, diagonal energies can always be expressed in terms of $v + \delta$, where δ is a Maslov index dependent on the dimensionality of the system. Similarly, the coupling matrix elements can be written in terms of scaled shift operators, a and $a^\dagger$, with matrix elements $\sqrt{v}\delta_{v',v-1}$ and $\sqrt{v+1}\delta_{v',v+1}$ respectively. There is also a widely used[3,4] semiclassical version of effective Hamiltonian theory, based on replacement of $v + \delta$ by the classical action I and of the shift operators by $\sqrt{I}e^{\pm i\alpha}$, where α denotes the classical angle variable conjugate to I.[5,6]

Such harmonic scaling rules permit the prediction of quantum and classical dynamics, for many systems, at any energy of interest. However real molecular vibrations always exhibit some degree of anharmonicity. Weakly anharmonic systems are commonly handled by "harmonically coupled anharmonic oscillator" theories which use Dunham expansions on the diagonal and harmonic shift operators for the off-diagonal coupling. No such harmonic oscillator based model can however cope with the extreme anharmonicity encountered when a Morse oscillator approaches dissociation or, even more severely, when a system approaches a saddle point.[7,8] Any accurate theory of resonant vibrational dynamics in regions of strong anharmonicity must utilize scaling rules that reflect the anharmonicity of the physical system.

The purpose of this paper is to lay the foundations for such a theory by pointing to the existence of remarkably accurate semiclassical scaling laws for the matrix elements. The aim is to provide scaling laws for strongly anharmonic zeroth-order models that can be used in place of the standard harmonic oscillator based theories. The simplest and most familiar zeroth-order model considered is the Morse oscillator, but we also introduce new scaling rules for two model systems with saddle points: a cylindrically symmetric double well (dubbed the "champagne bottle"[9]) and a planar or spherical pendulum.[10] The champagne bottle model applies, for example, to quasi-linear systems, such as the bending vibration of water, which can pass through linearity with eight vibrational quanta of excitation in the bending mode. The pendulum is relevant to systems which can undergo internal rotations, such as the bond-breaking internal rotation of HCP (rotation of H around the CP core) when the available bending/rotational energy exceeds ∼27 000 cm^{-1}.[11] Thus the results of this paper permit, for example, the derivation of scaling laws for a 2:1 resonance between Morse oscillators, or between a Morse oscillator an a symmetric double-well potential.

Each of the zeroth-order systems is expressed as a three-parameter model with a mass μ (or moment of inertia I in the case of the pendulum) and a potential function of the form $BV(ar)$ where B scales the energy and a the coordinate r. The theory employed involves angle-action transformations of the classical mechanics to obtain laws relating the scaled quantum numbers $(n + \delta)a/\sqrt{2\mu B}$ to the reduced energy E/B. Here δ is the Maslov index ($\delta = 0$, $^1/_2$, or 1 according to the dimensionality of the system). Expressions for representative coupling operators are then obtained in terms of the reduced energy and the classical angle variable. Finally the resulting formulas for the classical Fourier components are related to the quantal matrix elements, and shown to be remarkably accurate, by invoking the Heisenberg correspondence principle.[12] The present angle-action scaling rules are all analytical, though the corresponding quantal matrix are only analytical for the Morse oscillator; those for the systems with saddle points can only be determined numerically.

The basis of the correspondence principles and scaling laws are established in section II. Section III is concerned with the

* To whom correspondence should be addressed.
† Current address: Department of Chemistry, Columbia University, 3000 Broadway, MC 3158, New York, NY 10027.

10.1021/jp012582s CCC: $20.00
Published on Web 11/06/2001

Morse oscillator, while sections IV and V are devoted to the champagne bottle and spherical pendulum systems, respectively. Mathematical details of the angle-action transformations for the latter systems are covered in the Appendices. The conclusions are summarized in section VI.

II. Correspondence Principles and Scaling Laws

The fundamental classical/quantum correspondence relates the classical action I to the quantum number n by the equation[6,13]

$$I \simeq (n + \delta)\hbar \tag{1}$$

where $\delta = 0$ for rotation in a plane, $\delta = {}^1/_2$ for vibration or libration (e.g., orbital motion) and $\delta = 1$ for a two-dimensional isotropic oscillator. As an immediate consequence, the quantum mechanical eigenvalues may be approximated as

$$E_n \simeq H_{\rm cl}(I) = H_{\rm cl}[(n + \delta)\hbar] \tag{2}$$

while the local energy level separations are related to the classical frequencies $\omega = H_{\rm cl}/I$ by the equation

$$\frac{1}{2}(E_{n+1} - E_{n-1}) \simeq \frac{{\rm d}E_n}{{\rm d}n} = \frac{{\rm d}I}{{\rm d}n}\frac{\partial H_{\rm cl}}{\partial I} = \hbar\omega \tag{3}$$

Turning to the quantum mechanical matrix elements, there is no strict angle-action formulation of quantum mechanics,[14−16] but a systematic semiclassical theory[6] may be based on the existence of action operators

$$\hat{I} = \hbar\left(-i\frac{\partial}{\partial\alpha} + \delta\right) \tag{4}$$

where α is the classical angle conjugate to the action I. The notation α is preferred to the more common ϕ for this classical angle[5] to avoid later confusion with the spherical polar azimuthal angle. The eigenfunctions of $\hat{I}$ are clearly given by

$$\psi_n(\alpha) = \frac{1}{\sqrt{2\pi}}{\rm e}^{{\rm i}n\alpha} \tag{5}$$

which means that the matrix elements of an operator $\hat{A} = A(\hat{I},\alpha)$ may be expressed as

$$(n'|\hat{A}|n) \simeq \frac{1}{2\pi}\int_{-\pi}^{\pi} A(\bar{I},\alpha){\rm e}^{{\rm i}(n-n')\alpha}\,{\rm d}\alpha \tag{6}$$

in which $\bar{I}$ is an average action, which is taken for the scaling laws that follow as the action at the average energy $\bar{E} = (E_n + E_{n'})/2$. Equation 6 expresses the Heisenberg correspondence principle between quantal matrix elements and classical Fourier components.[12] The parentheses $(n'|\hat{A}|n)$ in eq 6 are used henceforth for the Fourier components and bracket combinations $\langle n'|\hat{A}|n\rangle$ for exact matrix elements.

The above results are particularly interesting for systems with three-parameter Hamiltonians of the form

$$H_{\rm cl} = \frac{1}{2\mu}p^2 + BV(ax) \tag{7}$$

where B and a^{-1} determine the energy and distance scaling of the potential function. The classical action then takes the form

$$I = \frac{1}{2\pi}\oint p(x)\,{\rm d}x = \frac{1}{\pi}\int_{x_-}^{x_+}\sqrt{2\mu[E - BV(ax)]}\,{\rm d}x \tag{8}$$

where $x_\pm$ are the classical turning points. The combination of eqs 1 and 8 implies that

$$(n + \delta)b = F(\epsilon) \tag{9}$$

where the reduced energy and action scaling parameters are given by

$$\epsilon = \frac{E}{B}, \quad b = \sqrt{\frac{a^2\hbar^2}{2\mu B}} \tag{10}$$

and

$$F(\epsilon) = \frac{1}{\pi}\int_{z_-}^{z_+}\sqrt{\epsilon - V(z)}{\rm d}z, \quad z = ax \tag{11}$$

Equation 9 implies that the scaled quantum number $(n + \delta)$-b is a universal function of the scaled energy ϵ for systems with the potential $BV(ax)$. Alternatively, by inverting eq 9,

$$E_n = Bf[(n + \delta)b] \tag{12}$$

where $f[(n + \delta)b]$ is the inverse function to $F(\epsilon)$. Taken together with eqs 3 and 6, these results imply that the quantum level separations and the quantum matrix elements scale simply with the reduced mean energy $\bar{\epsilon} = \bar{E}/B$, regardless of the precise mass μ and parameters B and a^{-1}, applicable to the situation in hand.

Similar arguments apply to separable systems, such as degenerate oscillators, with angular momentum. Suppose, for example, that

$$H_{\rm cl} = \frac{1}{2\mu}\left(p_{\rm r}^2 + \frac{p_\phi^2}{r^2}\right) + BV(ar), \quad p_\phi = m\hbar \tag{13}$$

It follows that

$$I_{\rm r} = \left(n_{\rm r} + \frac{1}{2}\right)\hbar = \frac{1}{\pi}\int_{r_-}^{r_+}\sqrt{2\mu\left\{E - BV(ar) - \frac{m^2\hbar^2}{2\mu r^2}\right\}}\,{\rm d}r \tag{14}$$

which rearranges to

$$\left(n_{\rm r} + \frac{1}{2}\right)b = F(\epsilon,mb) \tag{15}$$

where

$$F(\epsilon,mb) = \frac{1}{\pi}\int_{z_-}^{z_+}\sqrt{\left(\epsilon - V(z) - \frac{m^2b^2}{z^2}\right)}\,{\rm d}z \tag{16}$$

Here $z = ar$ while ϵ and b are again given by eq 10. Inversion of eq 16 implies that

$$E_{nr,m} = Bf\left[\left(n_{\rm r} + \frac{1}{2}\right)b,mb\right] \tag{17}$$

in which both $(n_{\rm r} + {}^1/_2)$ and m are scaled by the same parameter b, which may be regarded as a quantum capacity parameter. Formulas are given below to relate it to the quantum number at $E = B$ for the various model systems.

It should be noted in passing that $n_{\rm r}$ defined by eq 14 is the radial quantum number, related to the number of radial nodes in the wave function, or the quantum number $\upsilon_{\rm bent}$ in the literature on quasi-linear vibrations.[17] The quantum number υ

$= 2n_r + |m|$, which is employed for the pendulum model, corresponds to υ_{linear} in the terminology of Johns.[17]

III. Morse Oscillator

The case of a Morse oscillator is taken as a familiar introductory example. The Hamiltonian takes the form

$$H = \frac{1}{2\mu}p^2 + B[1 - e^{-ax}]^2 \tag{18}$$

(with B in place of the usual D for the sake of uniformity) and the scaled energy levels may be expressed as

$$\epsilon_n = \frac{E_n}{B} = 2\left(n + \frac{1}{2}\right)b - \left(n + \frac{1}{2}\right)^2 b^2 \tag{19}$$

where the parameter b is given by eq 10. Put in another way, b is related to the quantum number n^B at $E = B$ by $b = (n^B + {}^1/_2)^{-1}$. It is also readily verified that

$$\hbar\omega = \left(\frac{\partial E}{\partial n}\right) = 2bB\sqrt{1-\epsilon} \tag{20}$$

which confirms that the local level spacing scales as a function of the reduced energy.

The canonical transformation between position-momentum (x, p) and angle-action (I,α) variables[6] may also be expressed in terms of ϵ rather than I:

$$x = a^{-1}\ln\left(\frac{1 + \sqrt{\epsilon}\cos\alpha}{1-\epsilon}\right) \tag{21}$$

$$p = -\sqrt{2\mu B}\left(\frac{\sqrt{\epsilon(1-\epsilon)}\sin\alpha}{1 + \sqrt{\epsilon}\cos\alpha}\right) \tag{22}$$

It follows from eqs 6, 21, and 22 that the Fourier components of any power or combination of x, p, and the Morse variable $y = [1 - \exp(-ax)]$ may be expressed in terms of the parameters B and b, the average reduced energy ϵ, and the quantum number difference $n - n'$. For example,

$$\langle n + j|y|n\rangle = \delta_{0,j} - \frac{1}{2\pi}\int_{-\pi}^{\pi}\frac{(1-\epsilon)e^{-ij\alpha}}{1 + \sqrt{\epsilon}\cos\alpha}d\alpha = \delta_{0,j} + (-1)^{j+1}\sqrt{1-\epsilon}\left\{\frac{1-\sqrt{1-\epsilon}}{\sqrt{\epsilon}}\right\}^j \tag{23}$$

It may also be verified that the corresponding off-diagonal Fourier components of x, p, and y are related by

$$\langle n + j|y|n\rangle = a\sqrt{1-\epsilon}\langle n + j|x|n\rangle = \frac{i\langle n + j|p|n\rangle}{\sqrt{2\mu B}}, \quad j \geq 1 \tag{24}$$

The diagonal Fourier component of p vanishes and that of x is given by

$$\langle n|x|n\rangle = a^{-1}\ln\left(\frac{1 + \sqrt{1-\epsilon}}{2(1-\epsilon)}\right) \tag{25}$$

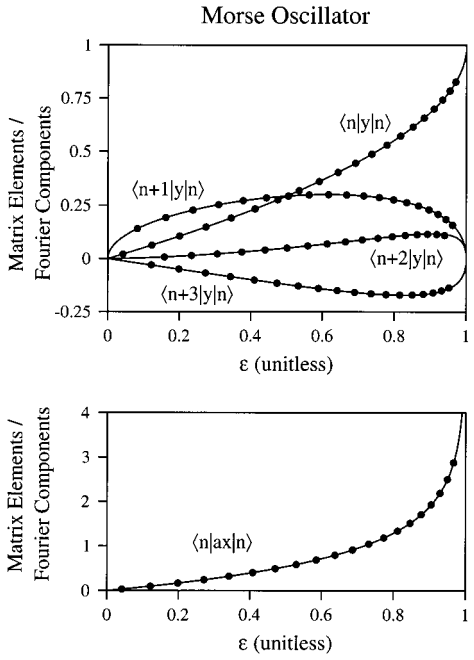

Figure 1. Matrix elements (points) and Fourier components (lines) of the Morse variable $y = 1 - e^{-ax}$ (upper) and of ax (lower). The quantum results are given for Morse parameters applicable to the OH local bond vibrations of H_2O, $\omega_e = 3874.62$, and $\omega_e x_e = 81.20$ cm^{-1}.

The upper part of Figure 1 shows the remarkable agreement between $\langle n'|y|n\rangle$ given by eq 23 and the corresponding exact quantum mechanical form[18]

$$\langle n + j|y|n\rangle = \delta_{0,j} + (-1)^{j+1}\sqrt{\frac{[n+j]!\Gamma(\gamma - n - j)(\gamma - 2n - 2j - 1)(\gamma - 2n - 1)}{n!\Gamma(\gamma - n)\gamma^2}} \tag{26}$$

where γ is related to the scaling parameter b of eq 10 by $\gamma = (2/b)$. The points are values of $\langle n + j|y|n\rangle$ plotted against the mean reduced energy $\bar{\epsilon} = (\epsilon_n + \epsilon_{n'})/2$ for the OH bond Morse parameters in a local mode model for H_2O,[19] namely, $\omega_e = 3874.62$ and $\omega_e x_e = 81.20$. The lines are the classical Fourier components given by eq 23.

A similar comparison is given in the lower part of Figure 1, between the above diagonal Fourier components and the quantal matrix elements[18]

$$\langle n|x|n\rangle = a^{-1}\ln\gamma + a^{-1}\sum_{m=0}^{n} C_m\{2[\psi^{(0)}(m+1) - \psi^{(0)}(1)] - \psi^{(0)}(\gamma - n - m - 1)\} \tag{27}$$

where $\psi^{(0)}$ is the digamma function $\psi^{(0)}(z) = \mathrm{d}\ln\Gamma(z)/\mathrm{d}z$[21] and

$$C_m = (\gamma - 2n - 1)\frac{n!\Gamma(\gamma - n - m - 1)}{(n-m)!\Gamma(\gamma - n)} \tag{28}$$

Note that the matrix elements of x, unlike those of y, become infinite as $\epsilon \rightarrow 1$. It is unnecessary to give other graphical comparisons because it may be verified, by use of the approximation

$$\sqrt{1-\epsilon} = 1 - \left(\bar{n} + \frac{1}{2}\right)\frac{\omega}{2B} \simeq \frac{\gamma - 2n - j - 1}{\gamma} \tag{29}$$

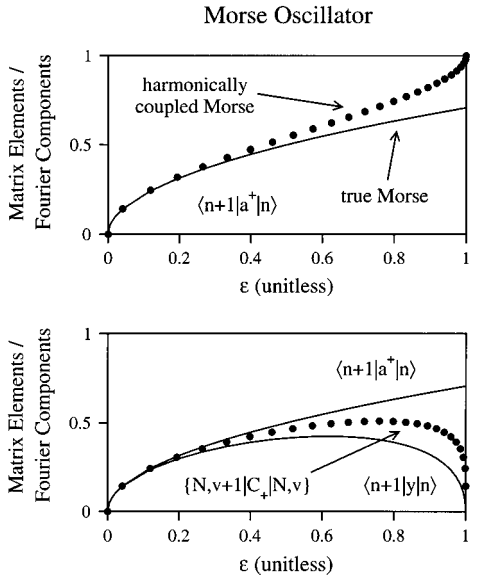

Figure 2. Comparison of $\Delta n = \pm 1$ matrix elements of various models. In the upper part, the semiclassical scaling for the Morse oscillator (specifically that of the creation operator, solid line) is compared with the predictions of a harmonically coupled Morse oscillator model (dots). In the lower part the vibron matrix elements $\sqrt{b}\{N,v+1|C_+|N,v\}$ are compared with the Morse oscillator Fourier components $\sqrt{b}(n+1|a^\dagger|n)$ (upper line) and $\sqrt{2}(n+1|y|n)$ (lower line). Parameter values were taken as $N + {}^1/_2 = b^{-1} = 24.5$.

that the known relationships between $\langle n'|y|n\rangle$, $\langle n'|x|n\rangle$, and $\langle n'|p|n\rangle$[18] are matched by the Fourier component identities in eq 24.

In view of the relevance to spectroscopic resonance models, it is also interesting to compare the $\Delta n = \pm 1$ Morse oscillator matrix elements with those of "harmonically coupled Morse oscillator"[19] and "vibron oscillator"[20] models. The former depend on the standard harmonic oscillator creation operator identity

$$\langle n+1|\,\hat{a}^\dagger|n\rangle = \left\langle n+1\left|\frac{1}{\sqrt{2\hbar}}\left(\sqrt{\mu\omega_e}x - i\frac{p}{\sqrt{\mu\omega_e}}\right)\right|n\right\rangle = \sqrt{\bar{n}+\frac{1}{2}} \quad (30)$$

where $\bar{n} = n + {}^1/_2$ is the mean quantum number. Bearing in mind that $\mu\omega_e = \sqrt{2\mu a^2 B}$ for the Morse oscillator, eqs 23 and 24 show that the corresponding Morse oscillator Fourier coefficient is given by

$$(n+1|\hat{a}^\dagger|n) = \left\langle n+1\left|\frac{1}{\sqrt{2\hbar}}\left(\sqrt{\mu\omega_e}x - i\frac{p}{\sqrt{\mu\omega_e}}\right)\right|n\right\rangle = \frac{\bar{\epsilon}}{2b} \quad (31)$$

where b is given by eq 10. In other words, within the validity of the correspondence principle, the true Morse matrix element of $\hat{a}^\dagger$ is proportional to the square root of the scaled mean energy $\bar{\epsilon}$ rather than that of the mean quantum number. The upper part of Figure 2 illustrates the difference between the forms in eqs 30 and 31 as a function of the reduced energy $\bar{\epsilon}$. The solid line shows the behavior of the true Morse Fourier component of $a^\dagger$, the open circles are the harmonic matrix elements $\langle n+1|\hat{a}^\dagger|n\rangle$. It is evident that "harmonically coupled anharmonic oscillator" models (open circles) significantly overestimate the true creation operator coupling (solid line) as soon as the energy exceeds 40% of the dissociation energy.

TABLE 1: Root Positions and Parameter Values for the Champagne Bottle ("champ") and Spherical Pendulum ("pend") in the Special Case $m = 0$

	z_1	z_2	z_3	k^2
$\epsilon_{champ} < 1$	$1+\sqrt{\epsilon}$	$1-\sqrt{\epsilon}$	0	$2\sqrt{\epsilon}/(1+\sqrt{\epsilon})$
$\epsilon_{champ} > 1$	$1+\sqrt{\epsilon}$	0	$1-<\sqrt{\epsilon}$	$(1+<\sqrt{\epsilon})/2\sqrt{\epsilon}$
$\epsilon_{pend} < 1$	1	$1-2\epsilon$	-1	ϵ
$\epsilon_{pend} > 1$	1	-1	$1-2\epsilon$	ϵ^{-1}

Finally, the vibron model employs states $|N,v\}$, with v running from 0 to N at the dissociation limit. The zeroth-order diagonal energies follow the Morse form in eq 19, with $N + {}^1/_2$ in place of b^{-1}, and the off-diagonal elements are given by

$$\{N,v+1|C_+|N,v\} = \sqrt{\frac{(\bar{v}+{}^1/_2)(N+{}^1/_2-\bar{v})}{(N+{}^1/_2)}}; \quad (32)$$

they clearly reduce to the harmonic form in the limit $\bar{v} \ll N$ but they fall off to $1/\sqrt{2}$ as $\bar{v} \rightarrow N$, instead of increasing monotonically with $\bar{v}$. In the lower part of Figure 2, the vibron matrix elements $\{N,v+1|C_+|N,v\}$ (filled circles, using $N = 24$) are compared with the Morse scaling $(n+1|\hat{a}^\dagger|n)$ [eq 31] and with the matrix element $(n+1|y|n)$ [eq 23]. The first two plots are multiplied by $\sqrt{b}$ and the second by $\sqrt{2}$ for scaling convenience. The comparison reveals no clear connection between the important $\Delta n = \pm 1$ matrix elements, except in the low ϵ limit. The vibron matrix elements (filled points) clearly correspond neither to the Morse oscillator creation/annihilation matrix elements (solid line) nor to the matrix elements of the variable $y = 1 - e^{-ax}$ (dashed line), which were chosen for comparison in view of the qualitatively similar falloff as $\epsilon \rightarrow 1$. Moreover, even if one could find more complicated operators with Morse matrix elements closer to the elements $\{N,v+1|C_+|N,v\}$, it is extremely unlikely that they would carry the vibron selection rule $\Delta n = \pm 1$. The upshot of this discussion is that there seems little benefit in trying to establish a close connection between the two types of theory. Morse oscillator methods have the benefit of a close connection with potential energy formulations of vibrational structure, while the vibron method is a more formal algebraic technique with particularly simple vibrational coupling rules.

IV. The Champagne Bottle

Details of the angle-action theory for the champagne bottle Hamiltonian

$$H_{champ} = \frac{1}{2\mu}\left(p_r^2 + \frac{p_\phi^2}{r^2}\right) + B(1-a^2r^2)^2 \quad (33)$$

are given in Appendix B for arbitrary angular momentum $p_\phi = m\hbar$. Results are given in terms of the roots z_i of the cubic polynomial equation

$$z^3 - 2z^2 + (1-\epsilon)z + m^2b^2 = 0 \quad (34)$$

and the combination

$$k^2 = \frac{z_1 - z_2}{z_1 - z_3} \quad (35)$$

where ϵ and b are given by eq 10, and the roots are ordered as $z_1 > z_2 > z_3$. Explicit formulas, given in Table 1, are available for the special case $m = 0$. Note that, although the functional forms are complicated, the z_i and k and thus the scaling rules

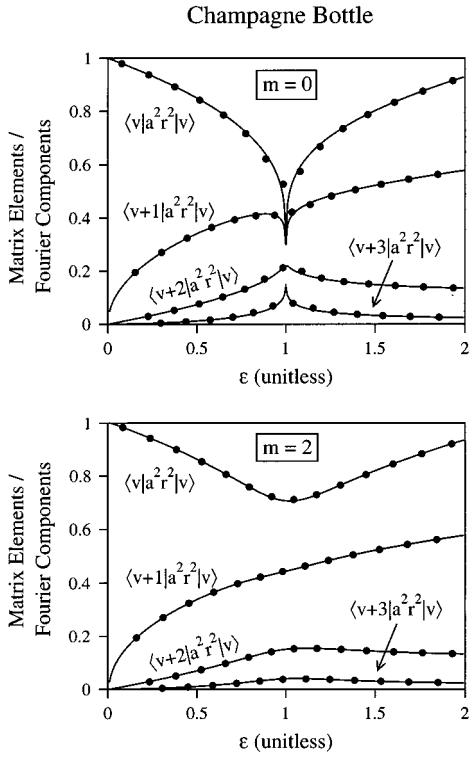

Figure 3. Matrix elements (points) and Fourier components (lines) of $(ar)^2$ for the champagne bottle with $m = 0$ (top) and with $m = 2$ (bottom). The quantum mechanical points were obtained from a model with $\mu = 1.78$ amu, $B = 11000$ cm^{-1}, and $a = 1.35$ Å^{-1}, roughly consistent with the bending motions of H_2O.

are uniquely determined by the reduced energy ϵ and the product mb. The quantum capacity parameter b itself may be shown, with the help of eqs B5−B7, to be related to the quantum number v_r^B at $E = B$ by

$$v_r^B + \frac{1}{2} = \frac{2\sqrt{2}}{3\pi b} \tag{36}$$

To take a concrete example, we can consider r to be a scaled bending variable approaching the bent to linear transformation in, for example, H_2O, and m to be the signed angular momentum around the a-axis (normally denoted k_a). The symmetry of such situations requires that any coupling must involve even powers of r. We therefore consider matrix elements of r^2 which are given according to eq B13 by

$$r^2 = a^{-2}\left[z_1 - (z_1 - z_2)\sum_{\mu=0}^{\infty} A_{2\mu}^{(2)}(k)\cos\mu\alpha_r\right] \tag{37}$$

where $A_{2\mu}^{(2)}(k)$ is given by eq A19. The Fourier components of r^2 therefore become

$$\begin{aligned}(v_r + \mu|r^2|v_r) &= a^{-2}[z_1 - (z_1 - z_2)A_0^{(2)}(k)] \quad \mu = 0\\ &= -\frac{1}{2a^2}(z_1 - z_2)A_{2\mu}^{(2)}(k) \quad \mu \neq 0\end{aligned} \tag{38}$$

Figure 3 shows the very close agreement between the classical Fourier components, given by eqs 38, and the quantum mechanical matrix elements of r^2, for a model with $v_r^B = 7.15$, obtained by a best fit to the calculated pure bending levels of H_2O,[22] with a barrier at $B = 11000$ cm^{-1}. Assuming a reduced mass for O and a pair of H atoms, $\mu = 1.78$ amu, this would imply $a = 1.35$ Å^{-1}, according to eqs 10 and 36. The mean value of ϵ, used for the quantum mechanical points, was taken as $\bar{\epsilon} = (E_{v_r+\mu} + E_{v_r})/2B$.

The general level of agreement between the quantum mechanical points and the classical lines is a remarkable testimony to the accuracy of the scaling laws, for a system whose classical motions experience dramatic changes on crossing the barrier at $E = B$. Minor discrepancies occur however in the immediate vicinity of the barrier maximum, $\epsilon = 1$, where the underlying Bohr quantization condition is known to require corrections.[6,9] Not surprisingly, the accuracy of the scaling is also seen to improve on passing from $m = 0$ to $m = 2$, because the semiclassical phase correction decreases with increasing m.[9] It should also be noted that the Fourier component plots for $m = 0$ are universal functions for all parameter sets (μ, a, B). However those for $m \neq 0$ must be computed for the appropriate composite quantum number, $b = a\hbar/\sqrt{2\mu B}$, because b appears in eq 34 for the roots z_i, and hence for the variable k, via eq 35.

V. Spherical Pendulum

Elements of the angle-action theory for the spherical pendulum, for which

$$H_{\text{pend}} = \frac{1}{2I}\left(p_\theta^2 + \frac{p_\phi^2}{\sin^2\theta}\right) + B\sin^2\frac{\theta}{2}, \quad p_\phi = m\hbar \tag{39}$$

are given in Appendix C. Results are given in terms of the roots z_i of the cubic polynomial equation

$$(2\epsilon - 1 + z)(1 - z^2) - m^2\beta^2 = 0 \tag{40}$$

and the combination

$$k^2 = \frac{z_1 - z_2}{z_1 - z_3} \tag{41}$$

where $\epsilon = E/B$ and $\beta = \hbar/\sqrt{IB}$. Table 1 gives expressions for the z_i and for k^2 in the special case $m = 0$.

As discussed in Appendix C, states are labeled by m and a quantum number v equivalent to that of a degenerate harmonic oscillator in the small amplitude limit. It follows from eq C8 that the capacity parameter, β, is related to v^B at $E = B$ by the identity

$$v^B + 1 = \frac{4\sqrt{2}}{\pi\beta} \tag{42}$$

We also recognize that motions coupled to the spherical pendulum must interact via even trigonometric functions of the angle θ. The function $\sin^2\theta$, which was taken earlier[10] as the leading term for Fermi resonance coupling to a stretching mode, is selected for illustrative purposes. Equations 6 and C11−C13 show that

$$(v + \mu|\sin^2\theta|v - \mu) = (1 - z_1^2)\delta_{\mu 0} + \frac{1}{2}(1 + \delta_{\mu 0})C_{2\mu} \tag{43}$$

where

$$C_{2\mu} = 2z(z_1 - z_2)A_{2\mu}^{(2)}(k) - (z_1 - z_2)^2 A_{2\mu}^{(4)}(k) \tag{44}$$

in which $A_{2\mu}^{(2)}(k)$ and $A_{2\mu}^{(4)}(k)$ are given by eqs A19 and A20.

The comparisons given in Figure 4 have the same qualitative character as those given for the champagne bottle in Figure 3. They relate to a previous study[10] with $\hbar^2/2I = 0.25$ and $B =$

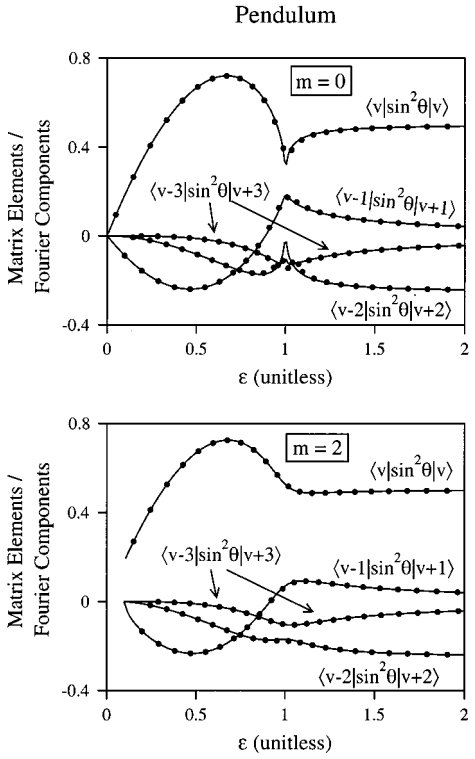

Figure 4. Matrix elements (points) and Fourier components (lines) of $\sin^2\theta$ for the spherical pendulum with $m = 0$ (top) and with $m = 2$ (bottom). The quantum mechanical points were obtained from a model with $B = 100$ and $\hbar^2/2I = 2$, both expressed in scaled energy units.

100 in a common system of energy units. Again there is a sharp break in the classical curves associated with drastic changes in the nature of the classical motions below and above the barrier at $E = B$. The changes are more strongly marked for $m = 0$, for which there is an unstable classical fixed point at the barrier maximum, than for $m = 2$. There is also again very close agreement between the lines marking the classical Fourier components and the points that represent the quantal matrix elements.

VI. Summary and Conclusions

The purpose of this paper is to demonstrate some remarkable scaling laws for the matrix elements of representative coupling operators between strongly anharmonic vibrational states. The rules follow from the correspondence principles between classical actions and quantum numbers, and between Fourier components and matrix elements. They are presented for three-parameter Hamiltonians characterized by a mass μ (or moment of inertia I) and a two-parameter potential of the form $BV(ax)$, in which case the reduced energy $\epsilon = E/B$ is found to be functionally dependent on the scaled action $Ia/\sqrt{2\mu B}$ and vice versa, where the functional form depends on the nature of $V(ax)$. Consequently *any* coupling function or operator, expressed in action-angles, can equally be expressed in terms of the reduced energy and the classical angles. It follows that the classical Fourier components may be treated as functions of the scaled energy ϵ. Thus, by the Heisenberg correspondence principle,[12] the same must be true for the quantum mechanical matrix elements.

Illustrations were provided for three strongly anharmonic oscillator systems: the Morse oscillator, a cylindrically symmetrical double well potential (champagne bottle) and the spherical pendulum (rotating over the surface of a sphere under a uniform field). In each case, remarkable quantitative agreement between classical and quantum results was found for the whole family of possible matrix elements. Figures 1−4 show at a glance how the magnitudes of the matrix elements vary with the reduced energy ϵ and with the quantum number change, Δn or Δv. The results are all expressed in analytical form, despite the fact that quantum mechanical treatments of the champagne bottle and the spherical pendulum can only be performed numerically. Moreover the scaling with reduced energy allows the presentation of all matrix elements for systems of the given type in a single diagram, regardless of the precise mass, energy, and length scale parameters for the physical problem under consideration.

The Morse oscillator example is relatively simple, because the results involve merely powers and square roots of familiar functions, which are simpler to visualize than the combinations of gamma functions that make up the exact matrix elements.[18] It was also possible to demonstrate the absence of any simple connection between Morse oscillator matrix elements and those employed in superficially similar vibron oscillator theories.[20] The champagne bottle and spherical pendulum models require more sophisticated analysis, much of which is placed in the Appendix. The results are typically expressed in terms of complete elliptic integrals, for which subroutines are available in *Numerical Recipes*.[23]

The results presented here suggest that the off-diagonal matrix elements (resonant interactions) in polyatomic molecule effective Hamiltonian models should be carefully parametrized to reflect the underlying dynamics, rather than parametrized in an ad hoc manner to reproduce eigenstate spectra. At energies well below dissociation or a saddle point, harmonic oscillator based effective Hamiltonian models may be appropriate, but care must be taken to ensure that the (off-diagonal) resonance scaling is consistent with the (diagonal) zeroth-order energy level spacings. By contrast, at energies approaching and exceeding a saddle point, harmonic oscillator based scaling rules break down catastrophically, and intrinsically anharmonic zeroth-order models must be used; no harmonic oscillator based theory can reproduce the cusps in Figures 3 and 4.

Although real molecular vibrations will not conform precisely to the above model systems, these systems undoubtedly provide better *zeroth-order* models for certain vibrational modes than the simple harmonic oscillator. Thus, it may prove possible to use perturbation theory to derive rapidly convergent effective Hamiltonians from one of our strongly anharmonic systems as a zeroth-order model. We suggest two possible approaches to directly fitting eigenstate spectra:

1. The analytical scaling rules derived above could provide a reasonable model for scaling the off-diagonal matrix elements, but higher order terms, essentially empirical in nature, could be added to the model diagonal energy terms to provide a better fit to experiment. This approach is conceptually analogous to the common harmonically coupled anharmonic oscillator model, except that one of our scaling systems replaces the harmonic oscillator as the zeroth-order model.

2. A more arbitrary zero-order model (for example a Fourier series, with the pendulum as the lowest order term) might be defined to reproduce the zeroth-order energy level spacings, after which numerical solution of the angle-action classical-mechanics for this potential could be used to generate matrix element scaling rules, in place of the analytical expressions presented here. Reference 24 gives an example of this approach.

Acknowledgment. M. P. J. and C. D. C. acknowledge financial support from the U.K. EPSRC.

Appendix A: Mathematical Preliminaries

The angle-action theory in the following sections makes use of Jacobian elliptic functions $sn(u,k)$, $cn(u,k)$, and $dn(u,k)$,[21,25,26] of which $sn(u,k)$ is implicitly defined by the equation

$$u = \int_0^{sn(u,k)} \frac{dt}{(1-t^2)(1-k^2t^2)}, \quad k^2 < 1 \tag{A1}$$

The nature of the integrand in eq A1 ensures that $sn(u,k)$ vanishes for $u = 0$, and reaches a maximum value of unity for real u, at which point

$$u = \int_0^1 \frac{dt}{(1-t^2)(1-k^2t^2)} = K(k) \tag{A2}$$

where $K(k)$ is the complete elliptic integral of the first kind. In the theory that follows, the variable u is proportional to the classical angle variable, and it will be useful to remember that $sn(u,k)$ is periodic in u with period $4K(k)$.

The functions $cn(u,k)$ and $dn(u,k)$ are related to $sn(u,k)$ by the equations

$$cn^2(u,k) = 1 - sn^2(u,k) \tag{A3}$$

$$dn^2(u,k) = 1 - k^2sn^2(u,k) \tag{A4}$$

from which it may be verified by differentiation of eq A2 that

$$\left(\frac{\partial sn}{\partial u}\right)_k = cn(u,k)dn(u,k) \tag{A5}$$

One convenient application of these Jacobian elliptic functions is for the evaluation of integrals involving square roots of cubic or quartic polynomials.[25,26] Suppose in the cubic case, which is relevant below, that the polynomial roots are ordered such that $z_1 > z_2 > z_3$ and that the integral is taken between z_2 and z_1. The substitution

$$z = z_1 - (z_1 - z_2)sn^2u \tag{A6}$$

leads with the help of eqs A3−A5 to

$$z_1 - z = (z_1 - z_2)sn^2u \tag{A7}$$

$$z - z_2 = (z_1 - z_2)cn^2u \tag{A8}$$

$$z - z_3 = (z_1 - z_3)dn^2u, \quad k^2 = (z_1 - z_2)/(z_1 - z_3) \tag{A9}$$

and

$$dz = -2(z_1 - z_2)snu\ cnu\ dnu \tag{A10}$$

Reference to the parameter k is suppressed in eqs A6−A10 but we note that $u = K(k)$ when $z = z_2$. It is readily verified with the help of eqs A3−A10 that

$$I_1 = \int_{z_2}^{z_1} \frac{dz}{\sqrt{(z_1 - z)(z - z_2)(z - z_3)}} = \frac{2}{\sqrt{(z_1 - z_3)}}\int_0^{K(k)} du = \frac{2K(k)}{\sqrt{(z_1 - z_3)}} \tag{A11}$$

One also finds by use of appropriate tables[25,26] that

$$I_2 = \int_{z_2}^{z_1} \frac{\sqrt{(z - z_3)}\,dz}{\sqrt{(z_1 - z)(z - z_2)}} = \sqrt{2(z_1 - z_3)}\int_0^{K(k)} dn^2u\,du = 2\sqrt{(z_1 - z_3)}E(k) \tag{A12}$$

and

$$I_3 = \int_{z_2}^{z_1} \frac{dz}{(z-p)\sqrt{(z_1 - z)(z - z_2)(z - z_3)}} = \frac{2}{\sqrt{(z_1 - z_3)}}\int_0^{K(k)} \frac{du}{1 - \alpha^2sn^2u} = \frac{2\Pi(\alpha^2,k)}{\sqrt{(z_1 - z_3)}} \tag{A13}$$

where

$$\alpha^2 = (z_1 - z_2)/(z_1 - p) \tag{A14}$$

The functions $E(k)$ and $\Pi(\alpha^2,k)$ in these equations are complete elliptic integrals of the second and third kinds[25,26] and the variable p in eqs A13−A14 is assumed to be distinct from the z_i. All other complete integrals involving the same cubic square roots may be reduced to combinations of I_1, I_2, and I_3. It will also be convenient to recognize that the incomplete form of I_1 above yields

$$\int_z^{z_1} \frac{dz}{\sqrt{(z_1 - z)(z - z_2)(z - z_3)}} = \frac{2u}{\sqrt{(z_1 - z_3)}} \tag{A15}$$

A second type of application stems from the fact that the Jacobian elliptic functions are doubly periodic in the complex variable u, with periods $4K(k)$ and $2iK'(k)$, where

$$K'(k) = K(\sqrt{1 - k^2}) \tag{A16}$$

The periodicity on the real u axis is of particular relevance, in view of the connection with classical angle variables. Fourier series for $sn(u,k)$, $cn(u,k)$, and $dn(u,k)$ are available in the literature,[21,25,26] and the following series for $sn^2(u,k)$ and $sn^4(u,k)$[10] will be useful later

$$sn^2(u,k) = \sum_{\mu=0}^{\infty} A_{2\mu}^{(2)}(k)\cos[\mu u\pi/K(k)] \tag{A17}$$

$$sn^4(u,k) = \sum_{\mu=0}^{\infty} A_{2\mu}^{(4)}(k)\cos[\mu u\pi/K(k)] \tag{A18}$$

where

$$A_{2\mu}^{(2)}(k) = \frac{2\pi^2}{k^2K^2(k)}\frac{\mu}{q^{\mu} - q^{-\mu}}, \quad \mu \neq 0$$

$$= \frac{1}{k^2K(k)}[K(k) - E(k)], \quad \mu = 0 \tag{A19}$$

$$A_{2\mu}^{(4)}(k) = \frac{\pi^2}{3k^4K^2(k)}\left[4(1+k^2) - \frac{\mu^2\pi^2}{K^2}\right]\frac{\mu}{q^{\mu} - q^{-\mu}}, \quad \mu \neq 0$$

$$= \frac{1}{3k^4K(k)}[(2+k^2)K(k) - 2(1+k^2)E(k)], \mu = 0 \tag{A20}$$

and

$$q(k) = \exp\left(\frac{-\pi K'(k)}{K(k)}\right) \tag{A21}$$

Appendix B: Angle-Action Theory for the Champagne Bottle

The champagne bottle Hamiltonian[9] may be expressed for present purposes in the form

$$H_{\text{champ}} = \frac{1}{2\mu}\left(p_r^2 + \frac{p_\phi^2}{r^2}\right) + B(1 - a^2r^2)^2 \tag{B1}$$

so that the radial action may be expressed as

$$\begin{aligned} J_r &= \left(v_r + \frac{1}{2}\right)\hbar = \frac{1}{2\pi}\oint p_r\, dr \\ &= \frac{\hbar}{2\pi b}\int_{z_2}^{z_1} \frac{\sqrt{\epsilon z - z(1-z)^2 - m^2b^2}}{z}\, dz \\ &= \frac{\hbar}{2\pi b}\int_{z_2}^{z_1} \frac{(z_1 - z)(z - z_2)(z - z_3)}{z\sqrt{(z_1 - z)(z - z_2)(z - z_3)}} dz \end{aligned} \tag{B2}$$

where ϵ and b are given by eq 10 and

$$z = (ar)^2 m = p_\phi/\hbar \tag{B3}$$

The z_i are roots of the polynomial equation

$$\epsilon z - z(1 - z)^2 - m^2b^2 = 0, \quad z_1 > z_2 > z_3 \tag{B4}$$

Substitution for z as given by eq A6, coupled with the identities[26]

$$j_1(k) = \int_0^K cn^2u\, dn^2u\, du = \frac{1}{3k^2}[(1 + k^2)E(k) - (1 - k^2)K(k)] \tag{B5}$$

$$j_2(\alpha^2,k) = \int_0^K \frac{cn^2u\, dn^2u}{1\text{-}\alpha^2 sn^2u} du = \frac{1}{\alpha^4}[\alpha^2E(k) + (\alpha^2 - 1)k^2K(k) + (\alpha^2 - 1)(\alpha^2 - k^2)\Pi(\alpha^2,k)] \tag{B6}$$

leads to

$$v_r + \frac{1}{2} = \frac{(z_1 - z_2)\sqrt{z_1 - z_3}}{\pi b}[j_2(\alpha^2, k) - j_1(k)] \tag{B7}$$

where

$$\alpha^2 = \frac{z_1 - z_2}{z_1} k^2 = \frac{z_1 - z_2}{z_1 - z_3} \tag{B8}$$

Notice that α^2 and k^2 depend, via the polynomial roots z_i, on the reduced energy ϵ, and the product mb. Consequently, eq B7 provides an implicit equation for the reduced energy in terms of mb and $(v_r + 1/2)b$.

The radial classical frequency ω_r, obtained by differentiation of eq B2 with respect to J_r, takes a simpler form because

$$\omega_r^{-1} = \left(\frac{\partial J_r}{\partial E}\right)_m = \frac{\hbar}{4\pi bB}\int_{z_2}^{z_1} \frac{dz}{\sqrt{(z_1 - z)(z - z_2)(z - z_3)}} = \frac{\hbar}{4\pi bB}\frac{2}{\sqrt{z_1 - z_3}}K(k) \tag{B9}$$

It remains to determine the classical angle α_r, conjugate to J_r, by differentiation of the classical generator

$$S = \int p_r\, dr + \int p_\phi\, d\phi \tag{B10}$$

with respect to J_r; thus, in the light of eqs A15, B1, and B3,

$$\alpha_r = \left(\frac{\partial S}{\partial J_r}\right) = \frac{\hbar}{4bB}\left(\frac{\partial E}{\partial J_r}\right)_m \int_z^{z_1} \frac{dz}{\sqrt{(z_1 - z)(z - z_2)(z - z_3)}} = \frac{\hbar}{4bB}\left(\frac{\partial E}{\partial J_r}\right)_m \frac{2u}{\sqrt{z_1 - z_3}} \tag{B11}$$

The combination of eqs B9 and B11 means that

$$\alpha_r = \frac{u\pi}{K} \tag{B12}$$

It therefore follows from eqs A6, A17, and B3 that

$$\begin{aligned} r^2 = a^{-2}z &= a^{-2}[z_1 - (z_1 - z_2)sn^2u] \\ &= a^{-2}[z_1 - (z_1 - z_2)\sum_{\mu=0}^{\infty} A_{2\mu}^{(2)}(k)\cos\mu\alpha_r] \end{aligned} \tag{B13}$$

Equation B13 provides the Fourier components required in section IV of the text.

Appendix C: Angle-Action Theory for the Spherical Pendulum

Details of the angle-action theory of the spherical pendulum, with the Hamiltonian

$$H = \frac{1}{2I}\left(p_\theta^2 + \frac{p_\phi^2}{\sin^2\theta}\right) + B\sin^2\frac{\theta}{2}, \quad p_\phi = m\hbar \tag{C1}$$

are given elsewhere.[10] The following summary, which is formulated from the elliptic function standpoint, is given to support the discussion in section V of the main text.

Integrals are cast into the forms in Appendix A by means of the substitution

$$\cos\theta = z = z_1 - (z_1 - z_2)sn^2u \tag{C2}$$

where the z_i are roots of the cubic equation

$$(a + z)(1 - z^2) - m^2\beta^2 = 0, \quad z_1 > z_2 > z_3 \tag{C3}$$

in which

$$a = \frac{2E}{B} - 1\ \beta^2 = \frac{\hbar^2}{IB} \tag{C4}$$

Notice that β differs from b in eq 10 because there is no formal range parameter in the potential, because the variable z lies in the dimensionless range $-1 < z < 1$. In view of the fact that

the small amplitude oscillations reduce to those of a degenerate harmonic oscillator, it is convenient to adopt a composite action

$$J_v = (v+1)\hbar = 2J_\theta + |J_\phi| \tag{C5}$$

where

$$v+1 = \frac{2}{\pi\beta}\int_{z_2}^{z_1} \frac{(a+z)(1-z^2) - m^2\beta^2}{1-z^2}\,\mathrm{d}z + |m|$$

$$= |m| + \frac{4}{\pi\beta\sqrt{z_1 - z_3}}\left[\int_0^{\mathrm{K}} \{(a+z_1) - (z_1 - z_2)sn^2u\}\,\mathrm{d}u \right. \tag{C6}$$

$$\left. - \frac{m^2\beta^2}{2}\int_0^{\mathrm{K}} \left\{\frac{1}{(z_1+1)(1-\alpha_+^2 sn^2u)} - \frac{1}{(z_1-1)(1-\alpha_-^2 sn^2u)}\right\}\mathrm{d}u\right]$$

$$\alpha_\pm^2 = \frac{z_1 - z_2}{z_1 \pm 1} \tag{C7}$$

It follows with the help of eqs A11−A13 that

$$v+1 = \frac{4}{\pi\beta\sqrt{z_1 - z_3}}\left[(a+z_3)K(k) + (z_1 - z_3)E(k) - \frac{m^2\beta^2}{2}\left\{\frac{\Pi(\alpha_+^2,k)}{(z_1+1)} - \frac{\Pi(\alpha_-^2,k)}{(z_1-1)}\right\}\right] + |m| \tag{C8}$$

where the parameter k is given by eq A9.

Expressions for the classical frequency, obtained by differentiation of eq C6 and of the classical generator, analogous to S in eq B10, are given by

$$\hbar\omega_v = \left(\frac{\partial E}{\partial v}\right)_m = \left[\frac{2}{\pi\beta B}\int_{z_2}^{z_1} \frac{\mathrm{d}z}{\sqrt{(z_1 - z)(z - z_2)(z - z_3)}}\right]^{-1} = \frac{\pi\beta B\sqrt{(z_1 - z_3)}}{4K(k)} \tag{C9}$$

and

$$\alpha_v = \frac{1}{\beta B}\left(\frac{\partial E}{\partial v}\right)_{\mathrm{m}} \int_{\mathrm{z}}^{z_1} \frac{dz}{\sqrt{(z_1 - z)(z - z_2)(z - z_3)}} = \frac{1}{\beta B}\left(\frac{\partial E}{\partial v}\right)_{\mathrm{m}} \frac{2}{\sqrt{(z_1 - z_3)}}\,u = \frac{u\pi}{2K(k)} \tag{C10}$$

The combination of eqs A17, A18, C2, and C10 means that

$$\cos\theta = z_1 - (z_1 - z_2)sn^2u$$

$$= z_1 - (z_1 - z_2)\sum_{\mu=0}^{\infty} A_{2\mu}^{(2)}(k)\cos[2\mu\alpha_{\mathrm{v}}] \tag{C11}$$

and it may also be verified that

$$\sin^2\theta = \sum_{\mu=0}^{\infty} C_{2\mu}\cos[2\mu\alpha_{\mathrm{v}}] \tag{C12}$$

where

$$C_{2\mu} = (1 - z_1^2)\delta_{\mu 0} + 2z_1(z_1 - z_2)A_{2\mu}^{(2)}(k) - (z_1 - z_2)^2 A_{2\mu}^{(4)}(k) \tag{C13}$$

References and Notes

(1) McCoy, A. B.; Sibert, E. L. *J. Chem. Phys.* **1996**, *105*, 459.
(2) Joyeux, M. *J. Chem. Phys.* **1998**, *109*, 2111.
(3) Xiao, L.; Kellman, M. E. *J. Chem. Phys.* **1990**, *90*, 5805.
(4) Xiao, L.; Kellman, M. E. *J. Chem. Phys.* **1990**, *90*, 5821.
(5) Goldstein, H. *Classical Mechanics*; Addison-Wesley: New York, 1980.
(6) Child, M. S. *Semiclassical Mechanics with Molecular Applications*; Oxford University Press: Oxford, U.K., 1991.
(7) Jacobson, M. P.; Field, R. W. *J. Phys. Chem. A* **2000**, *104*, 3073.
(8) Jacobson, M. P.; Jung, C.; Taylor, H. S.; Field, R. W. *J. Chem. Phys.* **1990** *111*, 600.
(9) Child, M. S. *J. Phys. A* **1998**, *31*, 657.
(10) Jacobson, M. P.; Child, M. S. *J. Phys. Chem. A* **2001**, *105*, 2834.
(11) Ishikawa, H.; Field, R. W.; Farantos, S. C.; Joyeux, M.; Koput, J.; Beck, C.; Schinke, R. *Annu. Rev. Phys. Chem.* **1999**, *50*, 443.
(12) Heisenberg, W. *Z. Phys.* **1925**, *33*, 879.
(13) Born, M. *Mechanics of the Atom*; Bell: London, 1960.
(14) Carruthers, P.; Nieto, M. M. *Rev. Mod Phys.* **1968**, *40*, 411.
(15) Leaf, B. *J. Math. Phys.* **1969**, *10*, 1980.
(16) Augustin, S. D.; Rabitz, H. *J. Chem. Phys.* **1979**, *71*, 4956.
(17) Johns, J. W. C. *Can. J. Phys.* **1967**, *45*, 2639.
(18) Sage, M. L. *Chem. Phys.* **1978**, *35*, 375.
(19) Halonen, L. *Adv. Chem. Phys.* **1998**, *104*, 41.
(20) Iachello, F.; Levine, R. D. *Algebraic Theory of Molecules*; Oxford University Press: New York, 1995.
(21) Abramowitz, M.; Stegun, I. A. *Handbook of Mathematical Functions*; Dover: New York, 1985.
(22) Partridge, H.; Schwenke, D. W. *J. Chem. Phys.* **1997**, *106*, 4618.
(23) Press, W. H.; Teukolsky, S. A.; Vetterling, W. T.; Flannery, B. P. *Numerical Recipes*, 2nd ed.; Cambridge University Press: Cambridge, U.K., 1992.
(24) Jacobson, M. P.; Child, M. S. *J. Chem. Phys.* **2001**, *114*, 262.
(25) Gradsteyn, I. S.; Ryzhik, I. M. *Tables of Integrals, Series and Products*, 5th ed; Academic Press: New York, 1994.
(26) Byrd, P. F.; Friedman, M. D. *Handbook of Elliptic Integrals for Engineers and Physicists*; Springer-Verlag: New York, 1954.